Dalton Transactions

Cite this: *Dalton Trans.*, 2011, **40**, 793

www.rsc.org/dalton

PAPER

Distinct structures of coordination polymers incorporating flexible triazole-based ligand: topological diversities, crystal structures and property studies†

Chen Ren, Lei Hou, Bin Liu, Guo-Ping Yang, Yao-Yu Wang* and Qi-Zhen Shi

Received 22nd July 2010, Accepted 6th October 2010
DOI: 10.1039/c0dt00894j

Six new coordination polymers, namely $\{[Zn(btec)_{0.5}(btmb)]\cdot 2H_2O\}_n$ (**1**), $\{[Co(btec)_{0.5}(btmb)(H_2O)]\cdot 3H_2O\}_n$ (**2**), $\{[Cu(btec)_{0.5}(btmb)]\cdot H_2O\}_n$ (**3**), $\{[Cu_4(btc)_4(btmb)_4]\cdot H_2O\}_n$ (**4**), $\{[Co_3(bta)_2(btmb)_2]\cdot 2H_2O\}_n$ (**5**), $[Co(Hbta)(btmb)]_n$ (**6**) (H_4btec = 1,2,4,5-benzenetetracarboxylate, H_3btc = 1,3,5-benzenetricarboxylate, H_3bta = 1,2,4-benzenetricarboxylate and btmb = 4,4′-bis(1,2,4-triazol-1-ylmethyl)biphenyl), have been successfully synthesized under hydrothermal conditions. All these complexes were structurally determined by single-crystal X-ray diffraction, elemental analysis, IR, TGA and XRD. Crystal structural analysis reveals that **1** is the first example of an unusual 3D framework with (8^6) topology containing a 2D molecular fabric structure. Complex **2** exhibits a 3D NbO network with ($6^4\cdot 8^2$) topology. In **3**, Cu(II) ions are coordinated by *anti*-conformational btmb ligands to form left- and right-handed double helices, which are further bridged by the 4-connected $btec^{4-}$ anions to give a 3D porous network. Complex **4** presents a rare 3D gra network structure with (6^3)($6^9\cdot 8$) topology. **5** and **6** were obtained through controllable pH values of solution, **5** features a scarce binodal (3,8)-connected tfz-d framework with the trinuclear Co(II) clusters acting as nodes, whereas **6** has an extended 2D 4^4 grid-like layer and the adjacent 2D layers are interconnected by strong hydrogen bonding interactions into a 3D supramolecular framework. The structural diversities indicate that distinct organic acid ligands, the nature of metal ions and the pH value play crucial roles in modulating the formation of the resulting coordination complexes and the connectivity of the ultimate topological nets. Moreover, magnetic susceptibility measurement of **5** indicates the presence of weak ferromagnetic interactions between the Co(II) ions bridged by carboxylate groups.

Introduction

The design and synthesis of functional metal–organic frameworks (MOFs) by the self-assembly of organic ligands with appropriate functional groups and metal ions acting as connecting nodes has attracted considerable interest, because of their intriguing variety of topologies and potential applications.[1–2] Up to now, the numerous studies devoted to the preparation of coordination polymers have been influenced by many factors, such as the metal-to-ligand molar ratio, the coordination geometry of the metal ions, the reaction temperature and the pH value of the solution *etc*.[3–4] In this field, organic ligands act as bridging linkers, which are of utmost importance because they greatly influence the overall framework of the coordination polymers in the self-assembly process. The partially or completely deprotonated forms of aromatic polycarboxylate ligands can adopt diverse binding modes and geometrical configurations to provide unique multidimensional structures and fascinating topologies. Some examples are 1,4-benzenedicarboxylate,[5] 1,3,5-benzenetricarboxylate,[6] 1,2,4-benzenetricarboxylate[7] and 1,2,4,5-benzenetetracarboxylate,[8] which have been extensively employed in the construction of interesting coordination polymers. The introduction of additional N-donor ligands to such synthetic systems can modify the structures and physical properties of the final materials. In this regard, flexible bis-imidazole or triazole ligands are good candidates for N-bridging ligands, which exhibit special abilities to formulate new coordination polymers with beautiful architectures and interesting properties.[9–10]

The flexible 1,2,4-triazole-containing 4,4′-bis(1,2,4-triazol-1-ylmethyl)biphenyl (btmb) ligand is also a good candidate, because the 1,2,4-triazole group exhibits strong coordination capacity

Key Laboratory of Synthetic and Natural Functional Molecule Chemistry of the Ministry of Education, Shaanxi Key Laboratory of Physico-Inorganic Chemistry, College of Chemistry and Materials Science, Northwest University, Xi'an 710069, P.R. China. E-mail: wyaoyu@nwu.edu.cn; Fax: +86-29-88303798

† Electronic supplementary information (ESI) available: Selected bond distances and angles (Table S1), TG and XRD patterns for complexes **1–6**. Additional crystallographic figures. CCDC reference numbers 785345–785350. For ESI and crystallographic data in CIF or other electronic format see DOI: 10.1039/c0dt00894j

and can provide more potential coordination sites, acting as a bridging ligand to produce targeted coordination polymers with fascinating architectures and multifunctional molecule materials.[11] In addition, two triazole groups can twist freely around two –CH_2– groups with different angles, to meet the requirement of the coordination geometries of the metal ions. So far, the coordination polymers constructed from the mixed flexible btmb and aromatic polycarboxylate ligands have rarely been investigated.[11]

On the basis of the aforementioned points, with the aim of further understanding the coordination chemistry of btmb and the influence of differently symmetrical polycarboxylate ligands on the formation of coordination polymers, herein, the simultaneous hydrothermal reaction of aromatic organic acids and long conformational bis-triazole ligand with metal ions affords six novel coordination polymers. These are $\{[Zn(btec)_{0.5}(btmb)]\cdot 2H_2O\}_n$ (**1**), $\{[Co(btec)_{0.5}(btmb)(H_2O)]\cdot 3H_2O\}_n$ (**2**), $\{[Cu(btec)_{0.5}(btmb)]\cdot H_2O\}_n$ (**3**), $\{[Cu_4(btc)_4(btmb)_4]\cdot H_2O\}_n$ (**4**), $\{[Co_3(bta)_2(btmb)_2]\cdot 2H_2O\}_n$ (**5**), $[Co(Hbta)(btmb)]_n$ (**6**) (H_4btec = 1,2,4,5-benzenetetracarboxylate, H_3btc = 1,3,5-benzenetricarboxylate and H_3bta = 1,2,4-benzenetricarboxylate). The thermal stabilities of these coordination complexes were discussed. Moreover, the photoluminescence property of **1** and magnetic property of **5** have also been investigated in detail.

Experimental

Materials and physical measurements

The 4,4′-bis(1,2,4-triazol-1-ylmethyl)biphenyl (btmb) ligand was synthesized according to the literature methods.[10d,11] All other starting materials were purchased from commercial sources, without further purification and used as received. Elemental analyses were recorded on a Perkin–Elmer model 240 C instrument. Mass spectra were determined with AXIMA-CFR™plus MALDI-TOF Mass Spectrometer mode. IR spectra were recorded with a Perkin–Elmer Spectrum One spectrometer in the region 4000–400 cm^{-1} using KBr pellets. Thermal analyses were performed on a NETZSCH STA 449 C microanalyzer with a heating rate of 10 °C min^{-1} under a N_2 atmosphere. The X-ray powder diffraction (XRD) data were recorded on a Rigaku RU200 diffractometer at 60 KV, 300 mA and Cu-Kα radiation (λ = 1.5406 Å), with a scan speed of 2° C min^{-1} and a step size of 0.02° in 2θ. Luminescence spectra for the solid samples were investigated with a Hitachi F-4500 fluorescence spectrophotometer at room temperature. The magnetic susceptibility of the microcrystalline sample restrained in parafilm was measured on a Quantum Design MPMS-XL7 SQUID magnetometer with an applied field of 1 kOe. Diamagnetic correction was estimated from Pascal's constants.

Preparation of complexes 1–6

Synthesis of $\{[Zn(btec)_{0.5}(btmb)]\cdot 2H_2O\}_n$ (1). The mixture of $Zn(NO_3)_2\cdot 6H_2O$ (0.0297 g, 0.1 mmol), H_4btec (0.0254 g, 0.1 mmol) and btmb (0.0316 g, 0.1 mmol) was dissolved in 12 mL of distilled water. The pH value was then adjusted to 6.0 with 1 M NaOH solution and the resulting mixture was transferred and sealed in a 25 mL Teflon-lined stainless steel vessel. This was then heated at 150 °C for 3 days and cooled to room temperature at 10 °C h^{-1}. Colourless crystals of **1** were collected in 51% yield (based on Zn). Elemental analysis (%) calcd for $C_{23}H_{21}ZnN_6O_6$: C 50.89, H 3.90, N 15.48. Found: C 50.73, H 3.83, N 15.86. IR (cm^{-1}): 357 m, 3126 m, 3100 m, 1669 s, 1594 s, 1544 w, 1496 w, 1382 s, 1272 m, 1129 s, 1074 w, 997 s, 832 m, 810 m, 754 s, 671 w, 640 m, 553 m.

Synthesis of $\{[Co(btec)_{0.5}(btmb)(H_2O)]\cdot 3H_2O\}_n$ (2). The preparation of **2** was similar to that of **1**, except $Co(CH_3COO)_2\cdot 4H_2O$ (0.0249 g, 0.1 mmol) was used instead of $Zn(NO_3)_2\cdot 6H_2O$. The pH value was then adjusted to 6.0 with 1 M NaOH solution. Pink crystals of **2** were collected in 68% yield (based on Co). Elemental analysis (%) calcd for $C_{23}H_{25}CoN_6O_8$: C 48.26, H 4.40, N 14.68. Found: C 48.29, H 4.53, N 14.59. IR (cm^{-1}): 3423 m, 3116 w, 2930 w, 1634 m, 1566 s, 1521 w, 1489 w, 1433 m, 1374 s, 1278 m, 1132 m, 1011 m, 986 w, 866 w, 811 m, 756 m, 676 m, 645 w, 581 w, 521 w.

Synthesis of $\{[Cu(btec)_{0.5}(btmb)]\cdot H_2O\}_n$ (3). The preparation of **3** was similar to that of **1**, except $Cu(NO_3)_2\cdot 4H_2O$ (0.0332 g, 0.1 mmol) was used instead of $Zn(NO_3)_2\cdot 6H_2O$. The pH value was then adjusted to 5.5 with 1 M NaOH solution. Blue crystals of **3** were collected in 42% yield (based on Cu). Elemental analysis (%) calcd for $C_{23}H_{19}CuN_6O_5$: C 52.82, H 3.66, N 16.07. Found: C 52.57, H 3.97, N 15.93. IR (cm^{-1}): 3440 s, 3128 m, 2926 w, 1629 m, 1584 s, 1540 m, 1486 m, 1363 s, 1285 m, 1206 w, 1124 s, 1043 w, 1002 m, 921 w, 891 w, 809 m, 752 m, 695 m, 599 w.

Synthesis of $\{[Cu_4(btc)_4(btmb)_4]\cdot H_2O\}_n$ (4). The preparation of **4** was similar to that of **3**, except H_3btc (0.0210 g, 0.1 mmol) was used instead of H_4btec. Only the pH value was then adjusted to 5.5 with 1 M NaOH solution. Blue crystals of **4** were collected in 40% yield (based on Cu). Elemental analysis (%) calcd for $C_{108}H_{76}Cu_4N_{24}O_{25}$: C 54.82, H 3.32, N 14.20. Found: C 54.39, H 3.14, N 14.35. IR (cm^{-1}): 3423 m, 3131 w, 3034 w, 1677 s, 1617 s, 1575 m, 1531 m, 1423 m, 1341 s, 1291 w, 1245 w, 1181 w, 1129 m, 1002 w, 841 w, 752 m, 720 m, 694 w, 628 w, 525 w.

Synthesis of $\{[Co_3(bta)_2(btmb)_2]\cdot 2H_2O\}_n$ (5). The preparation of **5** was similar to that of **2**, except H_3bta (0.0210 g, 0.1 mmol) was used instead of H_4btec. The pH value was then adjusted to 6.5 with 1 M NaOH solution. Pink crystals of **5** were collected in 70% yield (based on Co). Elemental analysis (%) calcd for $C_{54}H_{42}Co_3N_{12}O_{14}$: C 51.48, H 3.36, N 13.34. Found: C 51.39, H 3.34, N 13.04. IR (cm^{-1}): 3441 s, 3158 w, 3117 m, 1593 s, 1544 m, 1486 w, 1396 s, 1369 w, 1323 m, 1238 w, 1181 w, 1122 m, 1063 m, 1021 w, 813 m, 781 w, 675 w, 540 w.

Synthesis of $[Co(Hbta)(btmb)]_n$ (6). The preparation of **6** was similar to that of **2**, except H_3bta (0.0210 g, 0.1 mmol) was used instead of H_4btec. The pH value was adjusted to 5.0 with 1 M NaOH solution and pink crystals of **6** were collected in 30% yield (based on Co). Elemental analysis (%) calcd for $C_{27}H_{20}CoN_6O_6$: C 55.58, H 3.46, N 14.40. Found: C 55.39, H 3.69, N 14.34. IR (cm^{-1}): 3378 s, 3109 w,1567 s, 1435 w, 1379 s, 1277 w, 1182 w, 1128 m, 1076 w, 1017 m, 885 w, 851 w, 769 w, 756 m, 673 w, 642 w, 550 m, 501 w.

X-Ray crystallography

Single crystal X-ray diffraction analyses of the six complexes were carried out on a Bruker SMART APEX II CCD diffractometer equipped with a graphite monochromated Mo-Kα radiation (λ = 0.71073 Å) by using ϕ/ω scan technique at room temperature.

Table 1 Crystal data and structure refinements for complexes **1–6**[a]

Complexes	**1**	**2**	**3**	**4**	**5**	**6**
Formula	$C_{23}H_{21}ZnN_6O_6$	$C_{23}H_{25}CoN_6O_8$	$C_{23}H_{19}CuN_6O_5$	$C_{108}H_{78}Cu_4N_{24}O_{25}$	$C_{54}H_{42}Co_3N_{12}O_{14}$	$C_{27}H_{20}CoN_6O_6$
Formula mass	542.83	572.42	522.98	2366.11	1259.79	583.42
Crystal system	Monoclinic	Monoclinic	Monoclinic	Monoclinic	Triclinic	Orthorhombic
Space group	$P2_1/c$	$P2_1/c$	$C2/c$	$P2_1/c$	$P\bar{1}$	*Pnma*
a/Å	14.967(5)	15.237(7)	28.600(4)	10.1765(11)	9.301(2)	14.8802(15)
b/Å	14.962(5)	10.469(5)	11.5539(14)	16.4109(18)	10.576(3)	18.6040(19)
c/Å	10.836(4)	15.889(7)	17.686(2)	17.3490(17)	14.184(3)	9.5356(10)
α/°	90	90	90	90	86.683(3)	90
β/°	92.494(5)	91.075(7)	116.123(2)	119.258(2)	84.712(4)	90
γ/°	90	90	90	90	77.508(3)	90
V/Å^3	2424.4(14)	2534(2)	5247.3(11)	2527.8(4)	1355.4(6)	2639.8(5)
Z	4	4	8	1	1	4
D_c/g cm^{-3}	1.487	1.500	1.319	1.553	1.543	1.468
μ/mm^{-1}	1.064	0.737	0.884	0.921	0.986	0.704
F [000]	1116	1184	2128	1208	643	1196
θ/°	1.36–25.10	2.33–25.10	1.93–25.10	1.83–25.09	1.44–25.10	2.19–25.10
Reflections/unique collected	11 776/4298	12 342/4486	12 898/4664	12 407/4473	6861/4738	12 615/2429
Goodness-of-fit on F^2	1.033	1.008	1.029	1.037	1.046	1.040
Final R^a indices [$I > 2\sigma(I)$]	$R_1 = 0.0815$	$R_1 = 0.0642$	$R_1 = 0.0755$	$R_1 = 0.0462$	$R_1 = 0.0709$	$R_1 = 0.0597$
	$wR_2 = 0.1734$	$wR_2 = 0.1427$	$wR_2 = 0.2246$	$wR_2 = 0.1137$	$wR_2 = 0.1913$	$wR_2 = 0.1610$

[a] $R_1 = \Sigma(||F_o| - |F_c||)/\Sigma|F_o|$; $wR_2 = [\Sigma w(F_o^2 - F_c^2)^2/\Sigma w(F_o^2)^2]^{1/2}$.

All structures were solved by direct methods and refined by full-matrix least-squares fitting on F^2 by SHELX-97.[12] Absorption corrections were applied by using multi-scan program SADABS.[13] All of the nonhydrogen atoms were refined anisotropically. The hydrogen atoms of the organic ligands were refined as rigid groups. In **2**, the water hydrogen atoms of O6, O7 and O8 were located in difference Fourier maps and placed in calculated positions. Some of hydrogen atoms from the water molecules in complexes **1**, **3**, **4** and **5** could not be positioned reliably. In complex **3**, the two water O atoms, O5 and O6 were assigned 0.6 and 0.4 occupancies with no hydrogen atoms. Complex **4** has disordered free water molecule with the occupancy of 0.25. The results of TG and elemental analyses further confirmed the existence of water molecules in **3** and **4**. During refinement of the structure, some restraints were applied including distance restraints (DFIX) and thermal restraints (ISOR) which have been used on some unreasonable atoms in order to permit acceptable refinement of these parameters in complexes **1–6**.

The detailed crystallographic data and other pertinent information for complexes are summarized in Table 1. Selected bond lengths and angles are listed in Table S1.† Crystallographic data (excluding structure factors) for **1–6** have been deposited at the Cambridge Crystallographic Data Centre with CCDC reference numbers 785345–785350.

Results and Discussion

Syntheses

As is well known, the hydrothermal synthesis method has been demonstrated to be an effective and powerful technique for growing crystals of coordination polymers with interesting structural motifs and special properties. The construction of coordination polymers depends on the combination and careful control of many factors.[3–4] The control of the final product under hydrothermal reaction conditions is still a great challenge. We focus our attention on the employment of different aromatic polycarboxylate ligands (H_3btc, H_3bta and H_4btec), because differences in their size, their coordination ability, the number of carboxylate groups and the positions of the carboxylate groups may influence the framework of the final structure in the assembly process. In this study, it should be emphasized that the introduction of Zn(II), Co(II) and Cu(II) centre ions gave varied structures and topologies in **1–3**. When the pH value of the solvent was adjusted to 6.5 and 5.0, the H_3bta ligand shows different coordination modes in complexes **5** and **6**, respectively. All the complexes are air stable and insoluble in water or common organic solvents.

Structural description

$\{[Zn(btec)_{0.5}(btmb)]\cdot 2H_2O\}_n$ (1)

Single-crystal X-ray structural analysis reveals that **1** presents an interesting 3D network with a weave structure. The asymmetric unit is comprised of one Zn(II) ion, half of a btec^{4-} ligand, two half btmb ligands and two water solvent molecules. The half btec^{4-} ligand lies about an inversion centre, while the two half btmb ligands each lie about other independent inversion centres. As shown in Fig. 1a, each Zn(II) ion is coordinated by two carboxylic oxygen atoms from two different btec^{4-} anions (Zn–O = 1.931(6) and 1.945(6) Å) and two nitrogen atoms from two different btmb ligands (Zn–N = 2.010(8) and 2.007(7) Å), displaying a distorted tetrahedral environment, with all the bond lengths around the metal centres within the normal range.[8e] Each btec^{4-} anion adopts a μ_4 bridging mode to link four Zn atoms to form a sheet (Scheme 1a), leading to a 2D layer structure (Fig. 1b).[14] These adjacent 2D layers are further extended into 3D framework by *anti*-conformational btmb ligands. Each btmb ligand adopts an *anti*-configuration bridging mode to link the Zn(II) ions to form a 1D undulating chain with Zn···Zn distances of 17.071(9)–18.148(3) Å. However, it is fascinating that the crosslinking of adjacent 1D undulating $[Zn(btmb)]_n^{2-}$ chains *via*

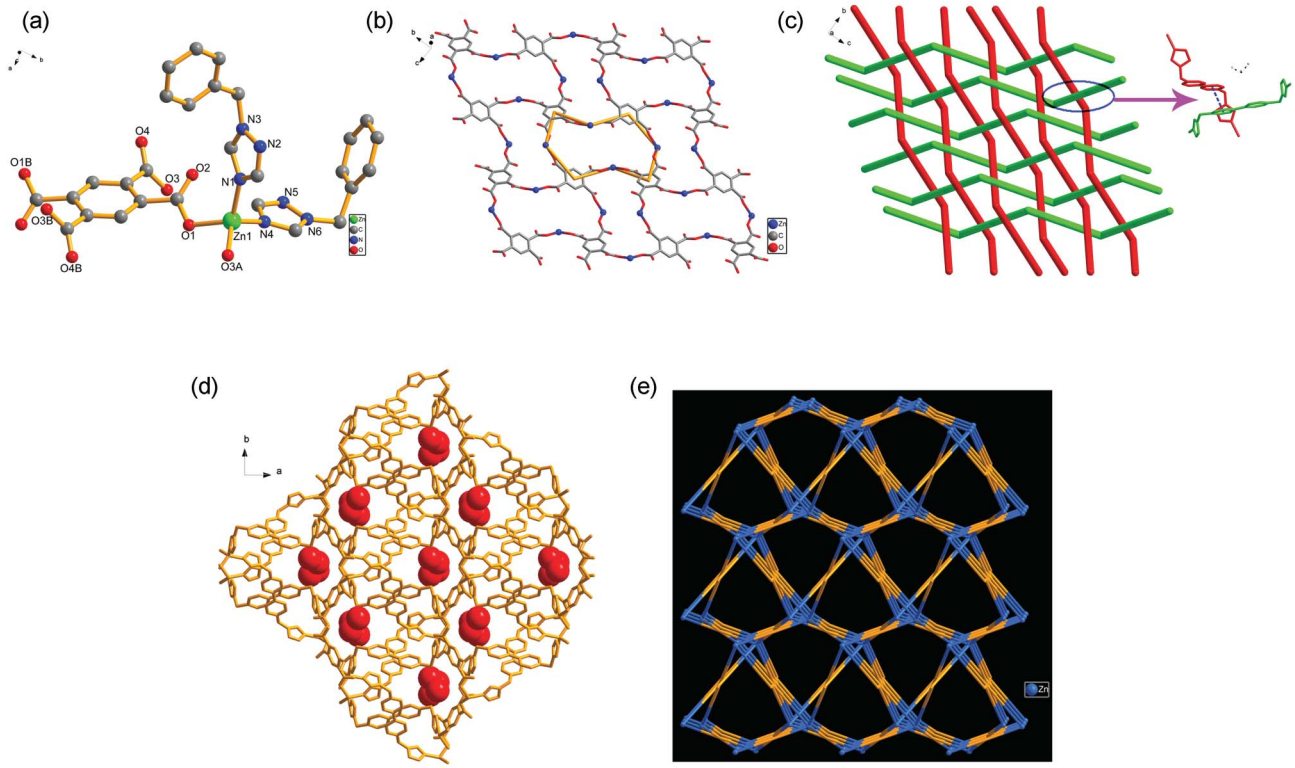

Fig. 1 (a) The coordination environment of the Zn(II) ions in **1**, water molecules have been omitted for clarity. Symmetry code: A = x, 0.5–y, 0.5+z, B = 2–x, –y, 1–z. (b) The 2D layer structure based on Zn(II) and 4-connected btec^{4-} anions. (c) View of the 2D (1O/1U) molecular fabric structure is formed by 1D undulating chains. (d) Perspective view of the 3D structure of **1** along the c axis, the red space filling model shows the channels with water molecules. (e) Schematic description of the 3D framework with (8^6) topology.

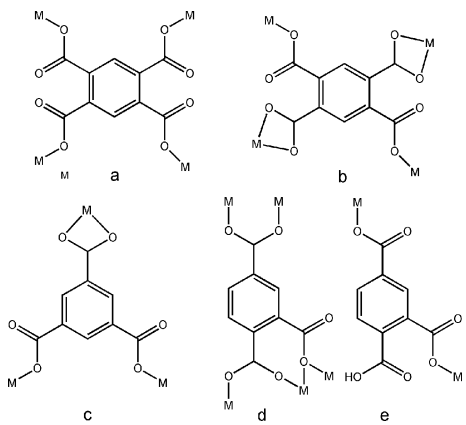

Scheme 1 The coordination modes of the aromatic carboxylic acids in complexes **1–6**.

weak π···π stacking interactions leads to a 2D "one-over/one-under"(1O/1U) molecular fabric structure (Fig. 1c), which is also observed in other 1D coordination polymers.[15] The weak π···π stacking interactions exist between the two phenyl rings, with a centre-to-centre distance of 4.056(6) Å, which stabilizes the crystal structure. To the best of our knowledge, these so-called fabric structures, which are interesting networks, are still surprisingly rare.[15]

In addition, there exist hydrogen bonding interactions between the free water molecules and the carboxylic oxygen atoms of the btec^{4-} anions (O5···O4#1 = 2.762(9) Å, O6···O5#2 = 2.958(5) Å, O6···O1#3 = 2.855(1) Å; #1 x, 1+y, z. #2 1–x, 1–y, –z. #3 –1+x, 0.5–y, –0.5+z), to further stabilize the resulting 3D framework (Fig. 1d). From the topological point of view, if the Zn(II) ions and btec^{4-} ligand are viewed as 4-connected nodes and btmb ligands are considered as linear linkers, the whole framework of coordination polymer **1** can be topologically considered as a scarce 3D framework with (8^6) net (Fig. 1e). Notably, this is the first example of a 3D coordination polymer containing weave structure with (8^6) topology.[16]

{[Co(btec)$_{0.5}$(btmb)(H$_2$O)]·3H$_2$O}$_n$ (2)

The asymmetric unit of **2** contains one Co(II) ion, half of a btec^{4-} ligand, one btmb ligand and four water molecules. The btec^{4-} ligand is generated by an inversion centre located in the middle of the aromatic ring and one of the four water molecules (O5) is directly bonded to the Co(II) centre. Each Co(II) ion adopts a distorted octahedral coordination geometry (Fig. 2a), which is coordinated by two nitrogen atoms from two btmb ligands (Co1–N1 = 2.098(4) and Co1–N4 = 2.143(4) Å), two oxygen atoms from one chelating carboxylate group (Co1–O1 = 2.189(3), Co1–O2 = 2.173(3) Å), one monodentate oxygen atom from a btec^{4-} ligand (Co1–O4 = 2.029(3) Å) and one coordinated water molecule (Co1–O5 = 2.045(4) Å). If the btmb ligand is neglected, each completely deprotonated btec^{4-} anion acts as a μ_4 bridging ligand, linking four Co(II) ions to build a 2D layer structure (Scheme 1b, Fig. 2b).[14] On the basis of this conductive way, these neighbouring 2D layers

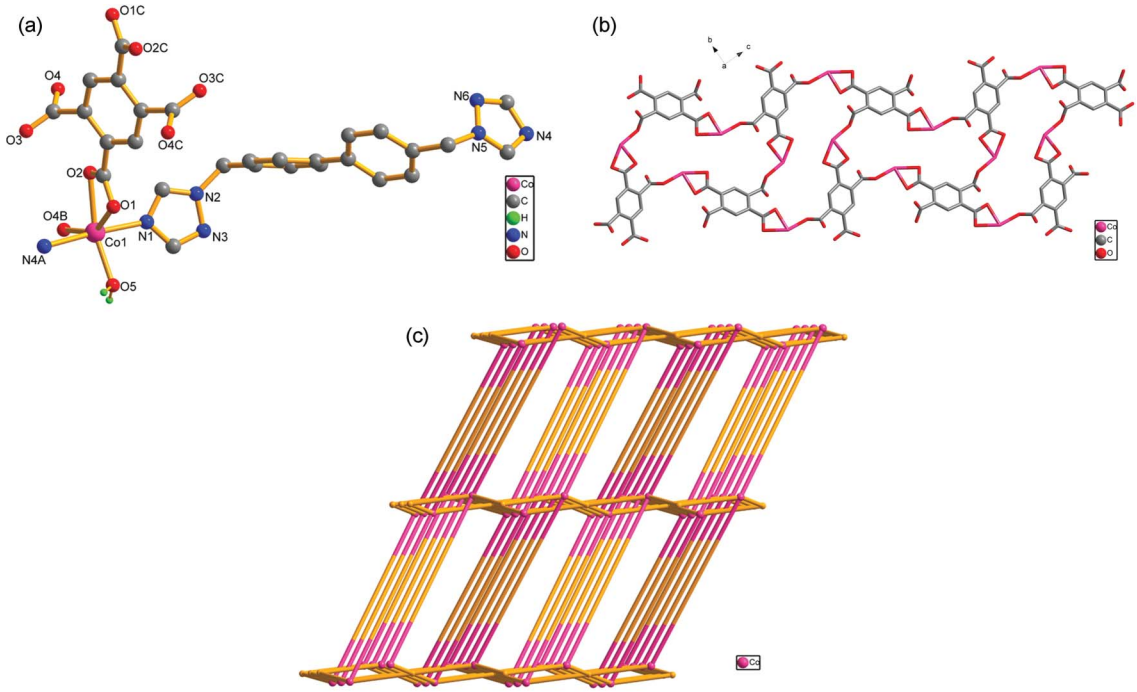

Fig. 2 (a) Perspective drawing of **2** showing the local coordination environment around the Co(II) ion. Symmetry code: A = −1+*x*, 0.5−*y*, −0.5+*z*, B = −*x*, −0.5+*y*, 0.5−*z*, C = −*x*, 1−*y*, 1−*z*. (b) View of 2D layer structure in **2**. (c) Schematic view of the topological framework of **2**.

are further connected together by btmb ligands to generate a 3D framework (Figure S1a†).

Water clusters $(H_2O)_n$ play an important role in crystallizing and stabilizing the conformation of the native crystal polymers, due to their ability to form hydrogen bonds with the host structure.[17] Interestingly, guest water molecules in **2** assemble themselves to form a water trimer, $(H_2O)_3$, through hydrogen bonding interactions with distances of 2.833(7) Å (O7···O6) and 2.929(2) Å (O6···O8), which is connected by O3 to give an infinite 1D chain (Figure S1b†). The bond angles of (O3···O7···O6), (O7···O6···O8), (O6···O8···O3) and (O8···O3···O7) are 139.46°, 98.09°, 116.87° and 115.74°, respectively. More noticeably, these intermolecular hydrogen bonding interactions further stabilize and strengthen the overall structure of complex **2**.

From the topological view, the $btec^{4-}$ anions and Co(II) centre can be considered as 4-connected nodes, the btmb ligand is simplified as a linker between the metal centres and the structure of **2** can be described as a 3D NbO network with $(6^4{\cdot}8^2)$ topology (Fig. 2c).[18]

$\{[Cu(btec)_{0.5}(btmb)(H_2O)]\cdot H_2O\}_n$ (3)

Single-crystal X-ray crystallography reveals that complex **3** represents a novel 3D porous coordination polymer, consisting of double helical chains with Cu(II)-btmb units. As shown in Fig. 3a, the half $btec^{4-}$ ligand lies about an inversion centre in the asymmetric unit, the Cu(II) centre represents a highly distorted octahedral coordination sphere that is defined by three oxygen atoms from two distinct $btec^{4-}$ ligands (Cu1–O1 = 1.978(4), Cu1–O2 = 2.626(8) and Cu1–O3 = 1.953(3) Å), one oxygen atom from a water molecule (Cu1–O5 = 2.799(5) Å) and two nitrogen atoms from two different btmb ligands (Cu1–N1 = 1.980(5), Cu1–N4 = 2.000(5) Å). However, the bond lengths of Cu1–O2 and Cu1–O5 are obviously longer than the normal range of the Cu–O bond, these are suggested to be non-negligible weak interactions between the metal centre and the oxygen atoms.[19] These weak interactions may play an important role in fixing the metal centres in a definite coordination geometry in **3**. Similarly to **2** (Scheme 1b), the four carboxylic groups of the fully deprotonated $btec^{4-}$ ligand exhibit two kinds of coordination modes. The $btec^{4-}$ ligand links copper ions to generate a 2D layer structure (Fig. 3b). More interestingly, Cu(II) ions are bridged by the *anti*-conformational btmb ligand to produce two kinds of 1D double helical chains (left- and right-handed) with a pitch of 23.10(7) Å (Fig. 3c). Two examples of double helical chains constructed with flexible btmb and bimb ligands have been reported previously (bimb = 4,4′-bis(1-imidazolyl)biphenyl).[9a,20] These 1D double helical chains are further superposed and interlinked by 4-connected $btec^{4-}$ anions, to generate a 3D porous framework (Fig. 3d). Notably, there exist weak hydrogen bonding interactions between O4, O5 and O6 (O···O = 2.889(0)–3.016(1) Å) from the host framework, which stabilize the whole crystal structure of **3**. When removing free water molecules, the effective free volume of **3** was calculated by PLATON analysis as 24.9% of the crystal volume (1305 $Å^3$ out of the 5247 $Å^3$ unit cell volume).[21]

In the view of topology, the simplified nodes of the Cu(II) centres and $btec^{4-}$ anions are the same as in complexes **1** and **2**. Hence, the overall framework for **3** can be regarded as a new 4-connected 3D network with Schläfli symbols $(6^2{\cdot}8^4)(6^4{\cdot}8^2)_2$ (Fig. 3e).

$\{[Cu_4(btc)_4(btmb)_4]\cdot H_2O\}_n$ (4)

When the symmetric H_4btec ligands are replaced by trigonal H_3btc ligands, a different 3D metal–organic framework **4** was obtained.

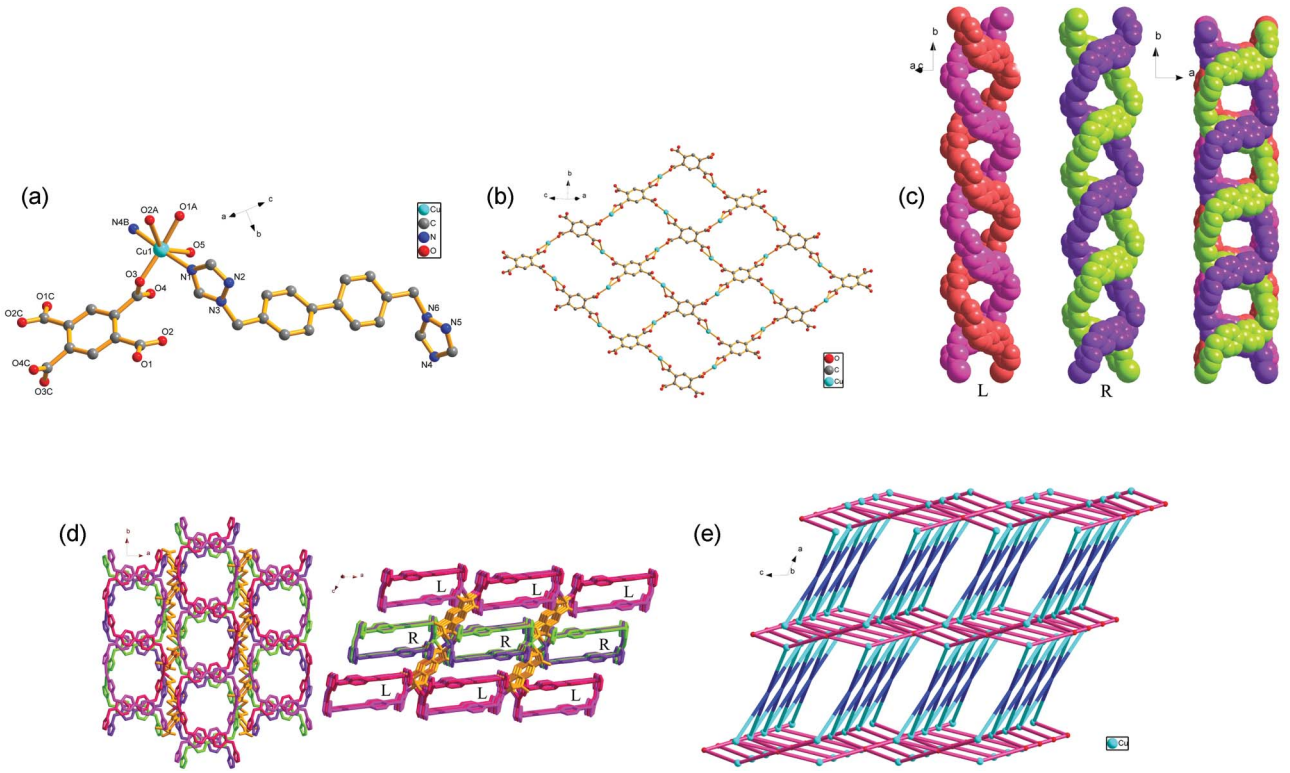

Fig. 3 (a) The coordination environment of the Cu(II) ion in **3**, all hydrogen atoms were omitted for clarity. Symmetry code: A = 0.5–*x*, –0.5+*y*, 0.5–*z*, B = –*x*, –1+*y*, 0.5–*z*, C = 0.5–*x*, 0.5–*y*, –*z*. (b) Schematic view of the 2D layer based on btec^{4-} anions and Cu(II) ions. (c) 1D double (left and right-handed) helical chains in **3**. (d) Schematic representation of the 3D framework and helical rectangular tubes of **3**. (e) Schematic view of the topological structure of **3**. The btmb linkers are shown as the two-coloured blue bonds.

The asymmetric unit of **4** consists of one Cu(II) ion and one btc^{3-} anion in general positions, two half btmb molecules each lying about independent inversion centres and a quarter of a free water molecule. Each Cu(II) centre displays an octahedral coordination geometry with two nitrogen atoms from two independent btmb ligands (Cu–N = 1.973(3) and 1.980(3) Å), four oxygen atoms from three different btc^{3-} anions (Cu1–O = 1.966(2), 1.972(2), 2.372(2) and 2.732(1) Å) (Fig. 4a). The longer Cu1–O3 bond is 2.732(1) Å, suggesting a non-negligible weak interaction which can be regarded as a semi-chelating coordination mode to stabilize the octahedral geometry of the Cu(II) centre.[4a] The completely deprotonated btc^{3-} anion displays bis-chelating and monodentate coordinated modes (Scheme 1c), in which each btc^{3-} anion can also be considered as a 3-connected node, to coordinate with Cu(II) ions to generate a 2D honeycomb network with (6,3) sheets (Fig. 4b).[22] These 2D frameworks are further linked by *anti*-conformational btmb ligands to form a 3D framework along the *a* axis (Figure S2†). Compared with other coordination polymers containing btmb ligands, a distinct 1D chain was formed by the metal centres and Z-shaped btmb ligands, without twisting the two phenyl rings (Fig. 4c).[11] In the view of topology, the Cu(II) centre and btc^{3-} ligand are regarded as 5- and 3-connected nodes and btmb ligand is considered as a linker, respectively. Therefore, the structure of **4** can be defined as a binodal (3,5)-connected 3D gra network with Schläfli symbols of $(6^3)(6^9{\cdot}8)$ (Fig. 4d). It should be emphasized that MOFs possessing a binodal (3,5)-connected framework are relatively rare, so far only a few coordination polymers with gra nets have been found.[23]

In the previous work, one 3D complex $[Cu_3(btc)_2(bimb)_2(H_2O)_3]_n$ was hydrothermally synthesized by incorporating a rigid imidazole-based spacer, bimb and a rigid aromatic 1,3,5-benzenetricarboxylate, which exhibits a trinodal 4-connected framework.[4a] Btmb is more flexible than the rigid bimb ligand. It generates the strong spacial tendency because of showing changeable conformational coordination modes with metal ions.[8d,9] Suitable steric geometry of the second ligands is also very important for the fabrication of the final coordination architectures.

$\{[Co_3(bta)_2(btmb)_2]\cdot 2H_2O\}_n$ (5)

Compared with complex **2**, in order to investigate the influence of asymmetrical phenyl polycarboxylic acid on the construction of coordination polymers, the highly asymmetrical H_3bta ligand was introduced, which leads to a new complex **5**. Significantly, it is interesting that btmb displays an asymmetrical *gauche* conformation with the different positions of the nitrogen atoms in **5** (See ESI†). There are two crystallographically independent Co(II) ions, both of which show distorted octahedral coordination geometries. It should be noted that the Co1 atom is in a general position in the asymmetric unit and the other Co2 atom lies on a crystallographic inversion centre. Each Co1 centre is coordinated by four oxygen atoms from three separated bta^{3-} anions (Co1–O1 = 2.049(4), Co1–O2 = 2.058(4), Co1–O3 = 2.164(4) and Co1–O5 = 2.064(4) Å) and two nitrogen atoms from two btmb ligands (Co1–N1 = 2.175(6) and Co1–N4 = 2.130(5) Å). Co2 is also

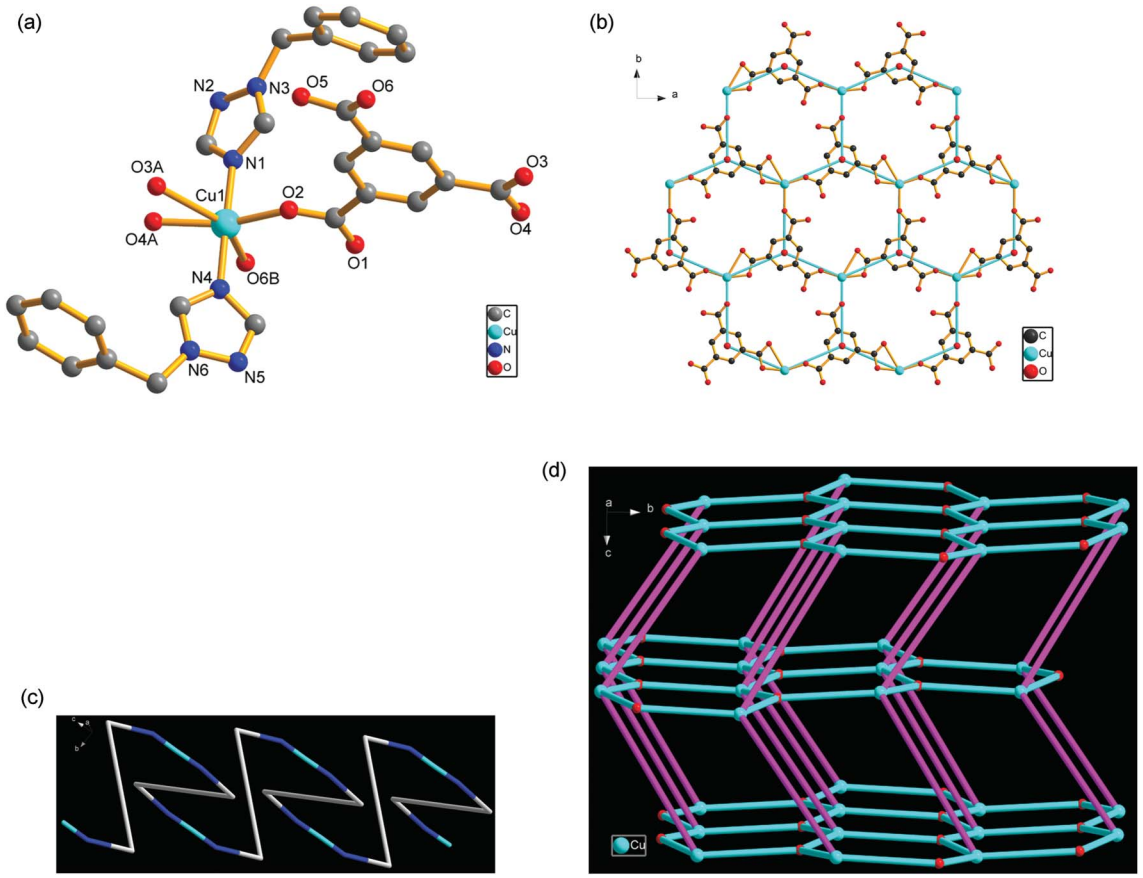

Fig. 4 (a) The coordination environment of the Cu(II) ion in **4**, all hydrogen atoms were omitted for clarity. Symmetry code: A = −1+*x*, *y*, *z*, B = 0.5−*x*, −0.5+*y*, 1.5−*z*. (b) View of the 2D layer with (6,3) sheets. (c) 1D chain based on Cu(II) ions and the btmb ligands. (d) Schematic representation of the (3,5)-connected 3D gra network with Schläfli symbols $(6^3)(6^9{\cdot}8)$ in **4**.

six-coordinated by four oxygen atoms from three bta^{3-} anions (Co2–O3 = 2.139(4) and Co2–O6 = 2.048(4) Å) and two nitrogen atoms from two btmb ligands (Co2–N5 = 2.150(5) Å) (Fig. 5a). As described in **1–4**, 1D chains are formed by bridging btmb ligands with bis-monodentate coordination mode. However, in the case of **5**, the asymmetrical btmb ligand adopts a tridentate coordination mode, which plays a 3-connected role in bridging Co(II) ions to generate a ladder-like chain (Fig. 5b). The bta^{3-} anion shows a μ_6 coordination mode (Scheme 1d)[24] and the Co(II) centres are interconnected by carboxylate groups to form a 2D layer structure, containing a trinuclear Co(II) cluster unit (Co1, Co2, Co1a) (Fig. 5c). The Co(II)···Co(II) distances are in the range of 3.514(9)–4.569(0) Å. These 2D layers are then pillared by flexible btmb spacers in two directions to generate a 3D framework with 1D water channels (Fig. S3†). After removal of the water molecules, PLATON analysis indicated that the effective free volume of **5** was 12.4% of the crystal volume (168 $Å^3$ out of the 1355 $Å^3$ unit cell volume).[21]

On the basis of the simplification principle, if the trinuclear Co(II) cluster unit is considered as an 8-connected single node, the bta^{3-} anion can be viewed as a 3-connected node and btmb ligand can be regarded as a linear linker between the trinuclear Co(II) clusters. Then the resulting structure of coordination polymer **5** can be classified as a unique binodal (3,8)-connected tfz-d framework with Schläfli symbols $(4^3)_2(4^6{\cdot}6^{18}{\cdot}8^4)$ (Fig. 5d),[25] which represents a new example of binodal high-connected MOFs in coordination chemistry frameworks.

[Co(Hbta)(btmb)]$_n$ (6)

When the hydrothermal reactions of H_3bta, btmb and cobalt salts were carried out at about pH value 5.0, a 2D grid-like layer structure of complex **6** was obtained. The asymmetric unit of **6** consists of one Co(II) ion, half of a btmb molecule and one $Hbta^{2-}$ anion. The Co(II) ion and $Hbta^{2-}$ ligand lie on a mirror plane with disorder of the carboxylic group and the half btmb ligand lies about an inversion centre in the asymmetric unit. As shown in Fig. 6a, the Co(II) ion shows a tetrahedral geometry, coordinated by two nitrogen atoms from two btmb ligands (Co1–N1 = 2.037(5) Å) and two oxygen atoms from two $Hbta^{2-}$ molecules (Co1–O = 1.909(5) and 1.976(4) Å). The Co(II) ions are bridged by *anti*-conformational btmb ligands to form a 1D infinite zigzag chain with a Co···Co distance of 18.256(0) Å, which is further interconnected through the bis-monodentate Hbta ligands (Scheme 1e) to generate a 2D undulating network with (4,4) sheets (Fig. 6b). In addition, the adjacent 2D undulating layer structures are parallel with each other and are extended by the strong hydrogen bonding interactions into a 3D supramolecular architecture (O3···O2 C = 2.495(7) Å. Symmetry code: C = 1/2+*x*, 1/2−*y*, 1/2−*z*) (Fig. 6c).

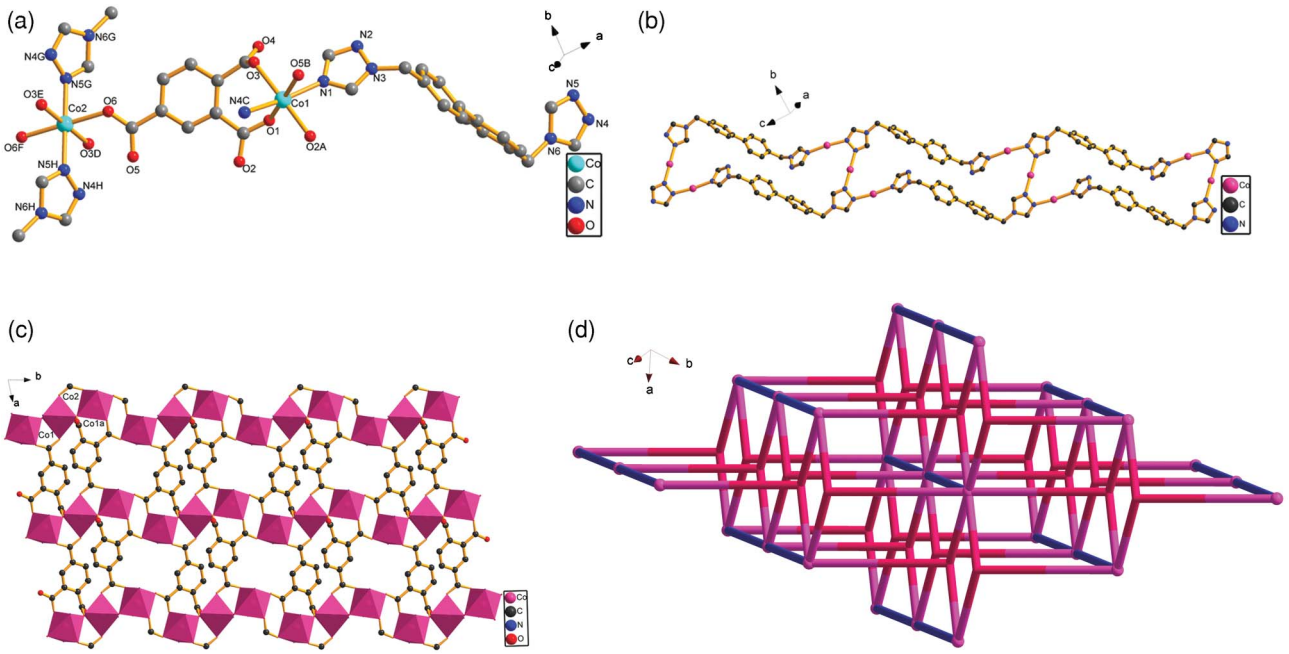

Fig. 5 (a) Coordination environment of the Co(II) ion in **5**, all hydrogen atoms were omitted for clarity. Symmetry code: A = 1–*x*, 2–*y*, 1–*z*, B = 1+*x*, *y*, *z*, C = –1+*x*, 1+*y*, 1+*z*, D = –1+*x*, *y*, *z*, E = –*x*, 3–*y*, 1–*z*, F = –1–*x*, 3–*y*, 1–*z*, G = 1–*x*, 2–*y*, –*z*, H = –2+*x*, 1+*y*, 1+*z*. (b) The 1D ladder-like chain was formed by btmb ligands and Co(II) ions. (c) View of the 2D network containing trinuclear Co(II) clusters. (d) Schematic view of the topology of **5**. Pink spheres represent trinuclear Co(II) cluster units, red nodes show bta^{3-} anions and btmb bridges are shown as blue linkers.

Comparison of the structures of coordination polymers

In the same synthetic conditions, the introduction of symmetrical and asymmetrical polycarboxylate ligands into the M(II)-btmb system affords diverse frameworks. In the 3D coordination complexes **1–3**, the highly symmetrical H_4btec ligand exhibits a μ_4 bridging mode to link the M(II) centres, to give 2D grid structures, which are extended into 4-connected topological frameworks through long flexible bis-triazole ligands. The different metal centres may be responsible for the structural diversities in **1–3**. Compared with the symmetrical H_4btec ligands, the unique three carboxylic groups of the asymmetrical H_3bta ligand offer more complicated coordination modes with the Co(II) ions, consequently resulting in the formation of a 3D (3,8)-connected architecture containing trinuclear Co(II) cluster units in **5**. Each fully deprotonated bta^{3-} anion adopts a μ_5 coordination mode with three carboxylate groups in μ_2-η^1:η^1, μ_2-η^2:η^1 and μ_2-η^1:η^1 bridging modes (Scheme 1d), respectively. In **3**, the $btec^{4-}$ anion adopts a μ_4 coordination mode and further connects the double helical chains to produce a 3D porous framework. Whereas in **4**, the incorporation of the C3-symmetric H_3btc ligand only results in a (3,5)-connected gra network, the deprotonated btc^{3-} ligand displays a μ_3 coordination mode to coordinate with the Cu(II) ions to generate 2D honeycomb network. Therefore, the comparison reveals that the steric geometry of the polycarboxylate ligands has a very significant effect on the formation and modulation of the final structures and topological nets. Highly asymmetrical carboxylate ligands possess a variety of coordination modes to produce unexpected architectures, as well as higher connected metal–organic frameworks.

In addition, the pH value of the solution may also influence the construction of the resulting frameworks.[3a,4b,4c] Complexes **5** and **6** were obtained under similar reaction conditions, but at different pH values, which were adjusted by the addition of 1M NaOH. In complexes **5** and **6**, the H_3bta ligand displays μ_6 and μ_2 bridging modes, respectively (Scheme 1d–e), it has been shown that an increase in the pH value results in a higher connectivity level of the bta^{3-} ligands, which in turn affects the formation of the high-dimensional reaction products and the topological networks.

Thermal stability analyses and X-ray power diffraction

To estimate the thermal stabilities of the six complexes, thermogravimetric analyses (TGA) experiments were carried out from 30 to 850 °C (Fig. S4†). The TGA curve of **1** shows that the first weight loss of 6.18% appeared from 60 to 120 °C, this corresponded to the loss of the two free lattice water molecules (calculated, 6.04%) and the second weight loss of 20.56% from 280 to 380 °C corresponded to the loss of the half btec molecule (calculated, 20.10%), the framework was then decomposed quickly resulting in the residue ZnO. For complex **2**, the first weight loss of 12.12% at 60–172 °C was consistent with the loss of the three lattice water molecules and the one coordinated water molecule (calculated, 12.59%). The resulting residue of complex **2** remains as CoO (calculated: 13.09%, found: 12.89%). For **3**, the weight loss from 40 to 166 °C was consistent with the loss of the free lattice water molecules. The observed weight loss of 3.98% is in agreement with the calculated 3.45%. At above 250 °C, the framework begins to decompose slowly and the remaining weight is attributed to the formation of CuO (calculated: 15.21%, found: 15.80%). In complex **4**, the first weight loss of is 1.01% in the temperature range of 60–82 °C, which corresponds to loss of the

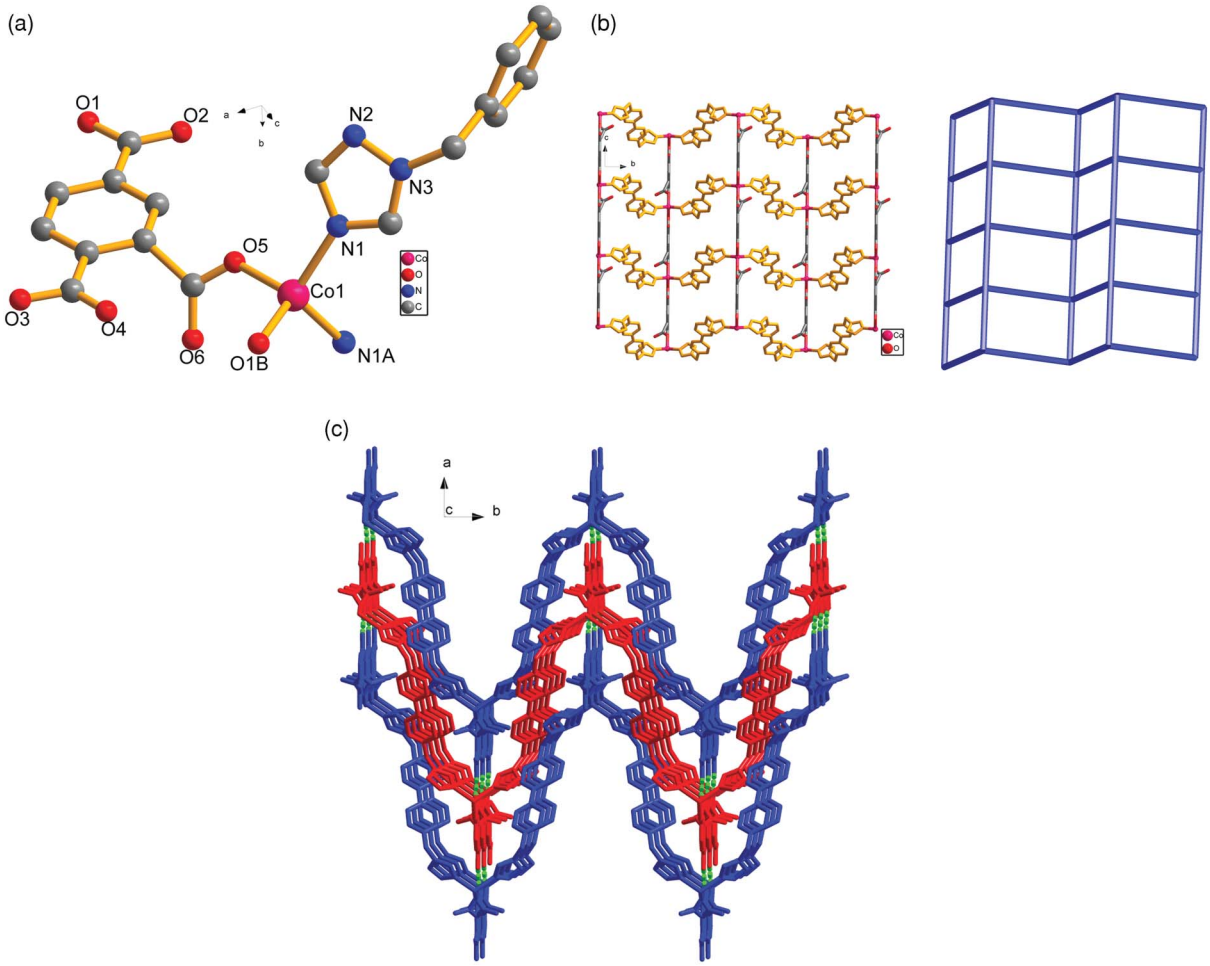

Fig. 6 (a) The coordination environment of the Co(II) ion in **6**, all hydrogen atoms were omitted for clarity. Symmetry code: A = x, 0.5–y, z, B = x, y, 1+z. (b) View of 2D undulating layer network with (4,4) sheets. (c) View of the 3D supramolecular framework is formed by the strong hydrogen bonding interactions (O3 ··· O2 C = 2.495(7) Å. Symmetry code: C = 1/2+x, 1/2–y, 1/2–z).

free water molecule (calculated: 0.76%). The second weight loss is 32.89% at 130–325 °C and the third weight loss is 52.67% in the temperature range of 326–700 °C, all assigned to the loss of organic ligands (calculated: 32.36% for H_3btc, 53.48% for btmb). The remaining weight, 14.02%, indicated that the final product was CuO (calculated: 13.45%). For complex **5**, there is an initial weight loss in the temperature range 40–130 °C, which arises from the loss of the water molecules (calculated: 2.86%, found: 2.87%). The second weight loss of 49.59% in the range of 227–441 °C may be assigned to the release of the btmb ligand and then the remaining weight, 19.00%, indicated that the remaining residue was Co_2O_3 (calculated: 19.75%). For **6**, the whole framework is stable up to 300 °C, from which point the composition of the framework begins to collapse and the remaining weight is attributed to the formation of CoO (calculated: 12.84%, found: 13.02%).

In order to characterize the phase purity of these complexes, X-ray power diffraction (XRD) patterns of complexes **1–6** were performed (Fig. S5†). Although minor differences can be observed in the positions, intensities and widths of some peaks, this shows that these complexes were obtained as a single phase. In complex **3**, After heating of the original sample at 150 °C for 5h, the guest water molecules were removed (Fig. S5c†). Diffraction intensity variations in the XRD patterns of **3** were observed, which may correspond to the loss of guest water molecules. No major differences are observed in the range 150–200 °C, which indicates that the framework of **3** is still maintained after removing the guest molecules. As shown in Fig. S5e,† the XRD of **5** was measured after heating at 100 °C, 150 °C and 220 °C, respectively. The results indicate that the overall framework of **5** is retained after the removal of the guest water molecule below 220 °C.

Luminescent properties

Functional coordination polymers, especially those with d^{10} metals complexes, have been investigated for their photoluminescent properties and potential applications.[26] As illustrated in Fig. S6,† the solid-state luminescent properties of complex **1** and the free btmb ligand were investigated at room temperature. An intense luminescent emission was observed at 400 nm (λ_{ex} = 280 nm) for complex **1** and at 352 nm (λ_{ex} = 280 nm) for the free btmb ligand. According to the previous studies, the free 1,2,4,5-benzenetetracarboxylic acid (H_4btec) exhibits one weak emission band at 342 (λ_{ex} = 308 nm).[14,27] Therefore, the emission of complex

1, with the enhancement of luminescence and red shift, may be assigned to the ligand-to-metal charge transfer (LMCT).[28]

Magnetic properties

A magnetic study has been performed on powdered samples of **5** at 1000 Oe in the range of 1.8–300 K. The χ_M and $\chi_M T$ *vs* T plots of **5** are shown in Fig. 7. The $\chi_M T$ value at 300 K is 9.63 cm^3 K mol^{-1}, which is higher than the expected value (5.64 cm^3 K mol^{-1}) of three spin-only Co(II) ions (S = 3/2, g = 2.0), indicating the important orbital contribution arising from the high-spin octahedral Co(II) centres.[29] As T is lowered, $\chi_M T$ continuously decreases and reaches a local minimum of 6.65 cm^3 K mol^{-1} at about 16 K, before increasing rapidly to a value of 9.89 cm^3 K mol^{-1} down to 1.8 K. The increase of $\chi_M T$ below 16 K suggests an appreciable ferromagnetic coupling between the Co(II) ions, which are connected to each other through μ_2-carboxylate and μ_2-carboxylate oxygen bridges.[29] The decrease of $\chi_M T$ in the range of 16–300 K is typical of spin–orbit coupling due to strong single-ion behaviour of Co(II).[4d] In order to estimate the strength of the ferromagnetic exchange interaction between Co(II) ions, the magnetic data of **5** were fitted using the simple phenomenological equation.[30]

$$\chi T = \mathrm{A}\exp(-E_1/kT) + B\exp(-\mathrm{E}_2/kT)$$

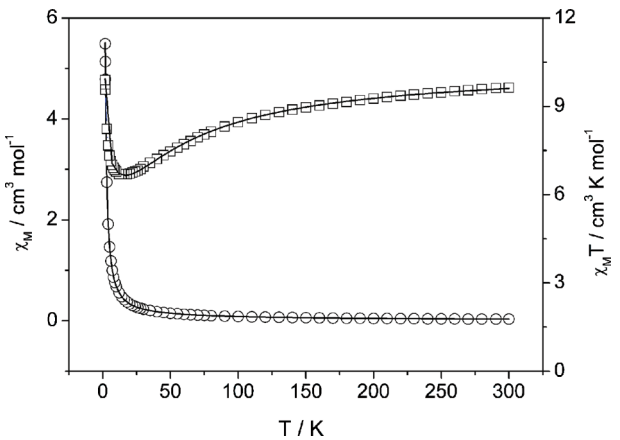

Fig. 7 $\chi_M T$ and χ_M plots for **5**.

The least-squares analysis ($R = 8 \times 10^{-4}$), shown as solid lines in Fig. 7, led to parameters A = 1.38 cm^3 mol^{-1} K, E_1/k = 65 K, B = 2.08 cm^3 mol^{-1} K and E_2/k = –0.84 K per Co(II). Here, A+B equals the Curie constant, and E_1 and E_2 represent the "activation energies" corresponding to the spin–orbit coupling and the magnetic exchange interaction. The Curie constant value found for A+B = 3.46 cm^3 mol^{-1} K, which agrees with that obtained from the Curie–Weiss law in the high temperature range and the value for E_1/k is consistent with those given in the literature for both the effects of spin–orbit coupling and site distortion (E_1/k of the order of 100 K). The value E_2/k = –0.84 K, corresponding to spin coupling between two Co(II) ions, shows the distinct ferromagnetic exchange mediated between Co(II) ions through μ_2-O and O–C–O bridges.

In order to estimate the spin–orbit coupling strength, the experimental data were fitted in eqn (1) by considering a mononuclear Co(II) with a spin–orbit coupling parameter λ in a molecular-field approximation.[31]

$$3\chi_{\mathrm{Co(II)}} = \frac{3N\beta^2}{k(T-\theta)x}\,\frac{\dfrac{7(3-A)^2x}{5} + \dfrac{12(A+2)^2}{25A} + \left\{\dfrac{2(11-2A)^2x}{45} + \dfrac{176(A+2)^2}{675A}\right\}\exp(-5Ax/2) + \left\{\dfrac{(A+5)^2x}{9} - \dfrac{20(A+2)^2}{27A}\right\}\exp(-4Ax)}{3 + 2\exp(-5Ax/2) + \exp(-4Ax)} \quad (1)$$

Where $x = \lambda/kT$, A is a crystal field parameter, λ is the spin–orbit coupling constant. The best fit gives the parameters A = 1.323, λ = 148 cm^{-1} and θ = 5.23 K (Fig. S7a†). The M *vs.* H at 1.8 K among 0–70 KOe is given in Fig. S7b,† which further confirms the expected ferromagnetic coupling between Co(II) centres in complex **5** (M = 7.00 Nβ) and the field dependence of the magnetization of **5** shows no hysteresis loop. Further, the AC magnetic susceptibility of **5** show that the in-phase (χ') magnetization increases with decreasing temperature, but no max peak was observed and the magnetization of out-phase (χ'') keeps constant within 0 K–50 K (Fig. S7c†) and suggests the absence of any magnetic ordering.[32]

Conclusions

In summary, a series of interesting coordination polymers have been hydrothermally synthesized by the combination of bis-triazole and rigid polycarboxylates ligands with metal ions. Complex **1** is the first example of a 3D framework containing weave structure with (8^6) topology. Complex **2** exhibits a 3D NbO network with ($6^4 \cdot 8^2$) topology. Complex **3** presents a novel 3D porous network consisting of double helical chains. Complex **4** shows a 3D gra network structure with (6^3)($6^9 \cdot 8$) topology, while complex **5** exhibits the rare (3,8)-connected tfz-d framework based on trinuclear Co(II) cluster units. Complex **6** has an undulating 2D 4^4 grid-like layer. Comparing the structures of these complexes, it is indicated that the distinct symmetry of organic acid anions, the nature of the metal ions and the pH value play crucial roles in modulating the formation of the final structures and topological nets. This work will not only deepen our systemic understanding of the structural functionality of the conformational flexibility of the btmb ligand but also provide new perspectives for generating metal–organic frameworks to enrich the field of crystal engineering. It is anticipated that more metal–organic frameworks containing conformational btmb ligands and carboxylate anions with intriguing structures and topologies as well as interesting physical properties will be synthesized.

Acknowledgements

We gratefully acknowledge financial support of this work by the National Natural Science Foundation of China (Grant No. 20771090), State Key Program of National Natural Science of China (Grant No. 20931005), Natural Science Foundation of Shaanxi Province (Grant No. 2009JZ001) and Specialized Research Found for the Doctoral Program of Higher Education (Grant No. 20096101110005).

References

1 (*a*) R. E. Morris and P. S. Wheatley, *Angew. Chem., Int. Ed.*, 2008, **47**, 4966; (*b*) S. S. Kaye, A. Dailly, O. M. Yaghi and J. R. Long, *J. Am. Chem. Soc.*, 2007, **129**, 14176; (*c*) M. Latroche, S. Surblé, C. Serre, C.

Mellot-Draznieks, P. L. Llewellyn, J.-H. Lee, J.-S. Chang, S. H. Jhung and G. Férey, *Angew. Chem., Int. Ed.*, 2006, **45**, 8227; (*d*) A. Corma, *Chem. Rev.*, 1997, **97**, 2373; (*e*) F. Schüth and W. Schmidt, *Adv. Mater.*, 2002, **14**, 629; (*f*) A. Stein, *Adv. Mater.*, 2003, **15**, 763.

2 (*a*) J. L. C. Rowsell and O. M. Yaghi, *Microporous Mesoporous Mater.*, 2004, **73**, 3; (*b*) M. P. Suh, Y. E. Cheon and E. Y. Lee, *Coord. Chem. Rev.*, 2008, **252**, 1007; (*c*) W. Lin, O. R. Evans, R. G. Xiong and Z. Wang, *J. Am. Chem. Soc.*, 1998, **120**, 13272; (*d*) J. Pang, E. J. P. Marcotte, C. Seward, R. S. Brown and S. N. Wang, *Angew. Chem., Int. Ed.*, 2001, **40**, 4042; (*e*) K. Inoue, H. Imai, P. S. Ghalsasi, K. Kikuchi, M. Ohba, H. Okawa and J. V. Yakhmi, *Angew. Chem., Int. Ed.*, 2001, **40**, 4242.

3 (*a*) H. Wang, Y. Y. Wang, G. P. Yang, C. J. Wang, G. L. Wen, Q. Z. Shi and S. R. Batten, *CrystEngComm*, 2008, **10**, 1583; (*b*) M. Munakata, L. P. Wu, T. Kuroda–Sowa, M. Maekawa, K. Moriwaki and S. Kitagawa, *Inorg. Chem.*, 1997, **36**, 5416; (*c*) Y. Suenaga, S. G. Yan, L. P. Wu, I. Ino, T. Kuroda–Sowa, M. Maekawa and M. Munakata, *J. Chem. Soc., Dalton Trans.*, 1998, 1121; (*d*) L. Carlucci, G. Ciani, D. W. V. Gudenberg, D. M. Proserpio and A. Sironi, *Chem. Commun.*, 1997, 631; (*e*) X. L. Wang, C. Qin, E. B. Wang and Z. M. Su, *Chem.–Eur. J.*, 2006, **12**, 2680.

4 (*a*) A. Y. Robin and K. M. Fromm, *Coord. Chem. Rev.*, 2006, **250**, 2127; (*b*) L. F. Ma, L. Y. Wang, D. H. Lu, S. R. Batten and J. G. Wang, *Cryst. Growth Des.*, 2009, **9**, 1741; (*c*) W. H. Zhang, Y. Y. Wang, E. K. Lermontova, G. P. Yang, B. Liu, J. C. Jin, Z. Dong and Q. Z. Shi, *Cryst. Growth Des.*, 2010, **10**, 76; (*d*) Y. Y. Liu, J. F. Ma, J. Yang and Z. M. Su, *Inorg. Chem.*, 2007, **46**, 3027; (*e*) J. Q. Liu, Y. N. Zhang, Y. Y. Wang, J. C. Jin, E. Kh. Lermontova and Q. Z. Shi, *Dalton Trans.*, 2009, 5365.

5 (*a*) Q. X. Yao, Z. F. Ju, X. H. Jin and J. Zhang, *Inorg. Chem.*, 2009, **48**, 1266; (*b*) J. H. Cavka, S. Jakobsen, U. Olsbye, N. Guillou, C. Lamberti, S. Bordiga and K. P. Lillerud, *J. Am. Chem. Soc.*, 2008, **130**, 13850; (*c*) L. Zhang, Z. J. Li, Q. P. Lin, Y. Y. Qin, J. Zhang, P. X. Yin, J. K. Cheng and Y. G. Yao, *Inorg. Chem.*, 2009, **48**, 6517; (*d*) B. Chen, X. Zhao, A. Putkham, K. Hong, E. B. Lobkovsky, E. J. Hurtado, A. J. Fletcher and K. M. Thomas, *J. Am. Chem. Soc.*, 2008, **130**, 6411; (*e*) P. Horcajada, C. Serre, G. Maurin, N. Ramsahye, A. F. Balas, M. Vallet-Regí, M. Sebban, F. Taulelle and G. Férey, *J. Am. Chem. Soc.*, 2008, **130**, 6774; (*f*) X. L. Wang, C. Qin, Y. Q. Lan, K. Z. Shao, Z. M. Su and E. B. Wang, *Chem. Commun.*, 2009, 410.

6 (*a*) L. L. Wen, F. Wang, J. Feng, K. L. Lv, C. G. Wang and D. F. Li, *Cryst. Growth Des.*, 2009, **9**, 3581; (*b*) C. D. Ene, A. M. Madalan, C. Maxim, B. Jurca, N. Avarvari and M. Andruh, *J. Am. Chem. Soc.*, 2009, **131**, 4586; (*c*) B. L. Chen, L. B. Wang, F. Zapata, G. D. Qian and E. B. Lobkovsky, *J. Am. Chem. Soc.*, 2008, **130**, 6718; (*d*) S. T. Zheng, J. Zhang and G. Y. Yang, *Angew. Chem., Int. Ed.*, 2008, **47**, 3909; (*e*) S. S. Y. Chui, S. M. F. Lo, J. P. H. Charmant, A. G. Orpen and L. D. Williams, *Science*, 1999, **283**, 1148; (*f*) R. E. Melendez, C. V. K. Sharma, M. J. Zaworkotko, C. Bauer and R. D. Togers, *Angew. Chem., Int. Ed. Engl.*, 1996, **35**, 2213.

7 (*a*) J. Yao, Z. D. Lu, Y. Z. Li, J. G. Lin, X. Y. Duan, S. Gao, Q. J. Meng and C. S. Lu, *CrystEngComm*, 2008, **10**, 1379; (*b*) P. Mahata, M. Prabu and S. Natarajan, *Inorg. Chem.*, 2008, **47**, 8451; (*c*) C. Qin, X. L. Wang, E. B. Wang, C. W. Hu and L. Xu, *Inorg. Chem. Commun.*, 2004, **7**, 788; (*d*) Y. Yan, C. D. Wu and C. Z. Lu, *Z. Anorg. Allg. Chem.*, 2003, **629**, 1991; (*e*) Y. Yan, C. D. Wu, X. He, Y. Q. Sun and C. Z. Lu, *Cryst. Growth Des.*, 2005, **5**, 821; (*f*) C. Qin, X. L. Wang, Y. G. Li, E. B. Wang, Z. M. Su, L. Xu and R. Clérac, *Dalton Trans.*, 2005, 2609; (*g*) L. Wang, M. Yang, Z. Shi, Y. Chen and S. H. Feng, *J. Solid State Chem.*, 2005, **178**, 3359.

8 (*a*) J. Y. Wu, M. T. Ding, Y. S. Wen, Y. H. Liu and K. L. Lu, *Chem.–Eur. J.*, 2009, **15**, 3604; (*b*) A. C. McKinlay, B. Xiao, D. S. Wragg, P. S. Wheatley, I. L. Megson and R. E. Morris, *J. Am. Chem. Soc.*, 2008, **130**, 10440; (*c*) O. Fabelo, J. Pasán, F. Lloret, M. Julve and C. Ruiz-Pérez, *Inorg. Chem.*, 2008, **47**, 3568; (*d*) O. Fabelo, J. Pasán, L. Cañadillas-Delgado, F. S. Delgado, F. Lloret, M. Julve and C. Ruiz-Pérez, *Inorg. Chem.*, 2008, **47**, 8053; (*e*) S. H. Huang, C. H. Lin, W. C. Wu and S. L. Wang, *Angew. Chem., Int. Ed.*, 2009, **48**, 6124.

9 (*a*) B. F. Hoskins, R. Robson and D. A. Slizys, *J. Am. Chem. Soc.*, 1997, **119**, 2952; (*b*) J. Yang, J. F. Ma, S. R. Batten and Z. M. Su, *Chem. Commun.*, 2008, 2233; (*c*) L. L. Wen, D. B. Dang, C. Y. Duan, Y. Z. Li, Z. F. Tian and Q. J. Meng, *Inorg. Chem.*, 2005, **44**, 7161; (*d*) L. Carlucci, G. Ciani and D. M. Proserpio, *Chem. Commun.*, 2004, 380; (*e*) J. Yang, J. F. Ma, Y. Y. Liu, J. C. Ma and S. R. Batten, *Cryst. Growth Des.*, 2008, **8**, 519; (*f*) Y. Qi, F. Luo, Y. X. Che and J. M. Zheng, *Cryst. Growth Des.*, 2008, **8**, 606; (*g*) J. Fan, G. T. Yee, G. Wang and B. E. Hanson, *Inorg. Chem.*, 2006, **45**, 599.

10 (*a*) Y. Q. Lan, S. L. Li, J. S. Qin, D. Y. Du, X. L. Wang, Z. M. Su and Q. Fu, *Inorg. Chem.*, 2008, **47**, 10600; (*b*) J. D. Lin, C. C. Jia, Z. H. Li and S. W. Du, *Inorg. Chem. Commun.*, 2009, **12**, 558; (*c*) B. F. Hoskins, R. Robson and D. A. Slizys, *Angew. Chem., Int. Ed. Engl.*, 1997, **36**, 2336; (*d*) X. R. Meng, Y. L. Song, H. W. Hou, H. Y. Han, B. Xiao, Y. T. Fan and Y. Zhu, *Inorg. Chem.*, 2004, **43**, 3528; (*e*) B. L. Li, Y. F. Peng, B. Z. Li and Y. Zhang, *Chem. Commun.*, 2005, 2333; (*f*) C. Qin, X. L. Wang, L. Yuan and E. B. Wang, *Cryst. Growth Des.*, 2008, **8**, 2093; (*g*) C. Qin, X. L. Wang, E. B. Wang and Z. M. Su, *Inorg. Chem.*, 2008, **47**, 5555.

11 (*a*) X. L. Wang, C. Qin, E. B. Wang and Z. M. Su, *Chem. Commun.*, 2007, 4245; (*b*) T. J. Ni, M. Shao, S. R. Zhu, Y. M. Zhao, F. F. Xing and M. X. Li, *Cryst. Growth Des.*, 2010, **10**, 943; (*c*) X. J. Shi, X. Wang, L. K. Li, H. W. Hou and Y. T. Fan, *Cryst. Growth Des.*, 2010, **10**, 2490; (*d*) Y. J. Mu, Y. J. Song, C. Wang, H. W. Hou and Y. T. Fan, *Inorg. Chim. Acta*, 2010, DOI: 10.1016/j.ica.2010.09.001.

12 G. M. Sheldrick, *SHELXL–97*, University of Göttingen, Germany, 1997.

13 G. M. Sheldrick, *SADABS 2.05,*University of Göttingen, Germany, 2002.

14 J. D. Lin, J. W. Cheng and S. W. Du, *Cryst. Growth Des.*, 2008, **8**, 3345.

15 (*a*) Y. H. Li, C. Y. Su, A. M. Goforth, K. D. Shimizu, K. D. Gray, M. D. Smith and H. C. Zur Loye, *Chem. Commun.*, 2003, 1630; (*b*) P. M. V. Calcar, M. M. Olmstead and A. L. Balch, *J. Chem. Soc., Chem. Commun.*, 1995, 1773; (*c*) A. M. P. Peedikakkal and J. J. Vittal, *Cryst. Growth Des.*, 2008, **8**, 375; (*d*) L. Carlucci, G. Ciani, A. Gramaccioli, D. M. Proserpio and S. Rizzato, *CrystEngComm*, 2000, 154; (*e*) P. M. V. Calcar, M. M. Olmstead and A. L. Balch, *Inorg. Chem.*, 1997, **36**, 5231.

16 (*a*) J. F. Ma, J. Yang, G. L. Zheng, L. Li and J. F. Liu, *Inorg. Chem.*, 2003, **42**, 7531; (*b*) M. L. Tong, X. M. Chen and S. R. Batten, *J. Am. Chem. Soc.*, 2003, **125**, 16170.

17 (*a*) J. M. Ugald, I. Alkorta and J. Elguero, *Angew. Chem., Int. Ed.*, 2000, **39**, 717; (*b*) R. Ludwig, *Angew. Chem., Int. Ed.*, 2001, **40**, 1808; (*c*) D. S. Li, Y. Y. Wang, X. J. Luan, P. Liu, C. H. Zhou, H. R. Ma and Q. Z. Shi, *Eur. J. Inorg. Chem.*, 2005, 2678; (*d*) F. N. Keutsch, J. D. Cruzan and R. J. Saykally, *Chem. Rev.*, 2003, **103**, 2533; (*e*) S. Pal, N. B. Sankaran and A. Samanta, *Angew. Chem., Int. Ed.*, 2003, **42**, 1741; (*f*) S. L. Li, Y. Q. Lan, J. C. Ma, J. F. Ma and Z. M. Su, *Cryst. Growth Des.*, 2010, **10**, 1161.

18 (*a*) L. Carlucci, N. Cozzi, G. Ciani, M. Moret, D. M. Proserpio and S. Rizzato, *Chem. Commun.*, 2002, 1354; (*b*) X. Lin, I. Telepeni, A. J. Blake, A. Dailly, C. M. Brown, J. M. Simmons, M. Zoppi, G. S. Walker, K. M. Thomas, T. J. Mays, P. Hubberstey, N. R. Champness and M. Schröder, *J. Am. Chem. Soc.*, 2009, **131**, 2159.

19 (*a*) W. Bidell, V. Shklover and H. Berke, *Inorg. Chem.*, 1992, **31**, 5561; (*b*) M. S. Wang, G. C. Guo, M. L. Fu, L. Xu, L. Z. Cai and J. S. Huang, *Dalton Trans.*, 2005, 2899; (*c*) F. He, M. L. Tong, X. L. Yu and X. M. Chen, *Inorg. Chem.*, 2005, **44**, 559; (*d*) Y. Wang, X. Q. Zhao, W. Shi, P. Cheng, D. Z. Liao and S. P. Yan, *Cryst. Growth Des.*, 2009, **9**, 2137.

20 S. L. Li, Y. Q. Lan, J. S. Qin, J. F. Ma, J. Liu and J. Yang, *Cryst. Growth Des.*, 2009, **9**, 4142.

21 A. L. J. Spek, *J. Appl. Crystallogr.*, 2003, **36**, 7.

22 (*a*) S. R. Batten, B. F. Hoskins, B. Moubaraki, K. S. Murray and R. Robson, *Chem. Commun.*, 2000, 1095; (*b*) W. X. Chen, S. T. Wu, L. S. Long, R. B. Huang and L. S. Zheng, *Cryst. Growth Des.*, 2007, **7**, 1171; (*c*) L. P. Zhang, J. Yang, J. F. Ma, Z. F. Jia, Y. P. Xie and G. H. Wei, *CrystEngComm*, 2008, **10**, 1410.

23 (*a*) I. A. Baburin, V. A. Blatov, L. Carlucci, G. Ciani and D. M. Proserpio, *Cryst. Growth Des.*, 2008, **8**, 519; (*b*) L. Hou, J. P. Zhang and X. M. Chen, *Cryst. Growth Des.*, 2009, **9**, 2415; (*c*) M. O'Keeffe, M. A. Peskov, S. J. Ramsden and O. M. Yaghi, *Acc. Chem. Res.*, 2008, **41**, 1782; (*d*) R. Heck, J. Bacsa, J. E. Warren, M. J. Rosseinsky and D. Bradshaw, *CrystEngComm*, 2008, **10**, 1687; (*e*) D. Kong, J. Zon, J. McBee and A. Clearfield, *Inorg. Chem.*, 2006, **45**, 977.

24 Z. L. Lu, W. Chen, J. Q. Xu, L. J. Zhang, C. L. Pan and T. G. Wang, *Inorg. Chem. Commun.*, 2003, **6**, 244.

25 (*a*) G. H. Wang, Y. Q. Lei, N. Wang, R. L. He, H. Q. Jia, N. H. Hu and J. W. Xu, *Cryst. Growth Des.*, 2010, **10**, 534; (*b*) S. J. Garibay, J. R. Stork, Z. Q. Wang, S. M. Cohen and S. G. Telfer, *Chem. Commun.*, 2007, 4881; (*c*) M. O'Keeffe, M. A. Peskov, S. J. Ramsden and O. M. Yaghi, *Acc. Chem. Res.*, 2008, **41**, 1782; (*d*) G. J. Xu, Y. H. Zhao, K. Z. Shao, Y. Q. Lan, X. L. Wang, Z. M. Su and L. K. Yan, *CrystEngComm*, 2009, **11**, 1842.

26 (*a*) Q. Wu, M. Esteghamatian, N. X. Hu, Z. D. Popovic, G. Enright, Y. Tao, M. D'Iorio and S. Wang, *Chem. Mater.*, 2000, **12**, 79; (*b*) G. De.

Santis, L. Fabbrizzi, M. Licchelli, A. Poggi and A. Taglietti, *Angew. Chem., Int. Ed. Engl.*, 1996, **35**, 202; (*c*) U. H. F. Buna, *Chem. Rev.*, 2000, **100**, 1605; (*d*) G. Yu, S. Yin, Y. Liu, Z. Shuai and D. Zhu, *J. Am. Chem. Soc.*, 2003, **125**, 14816; (*e*) W. Chen, J. Y. Wang, C. Chen, Q. Yue, H. M. Yuan, J. S. Chen and S. N. Wang, *Inorg. Chem.*, 2003, **42**, 944.

27 Y. Hou, S. T. Wang, E. H. Shen, E. B. Wang, D. R. Xiao, Y. G. Li, L. Xu and C. W. Hu, *Inorg. Chim. Acta*, 2004, **357**, 3155.

28 S. L. Zheng, J. P. Zhang, X. M. Chen, Z. L. Huang, Z. Y. Lin and W. T. Wong, *Chem.–Eur. J.*, 2003, **9**, 3888.

29 (*a*) P. Lama, A. Aijaz, E. C. Sañudo and P. K. Bharadwaj, *Cryst. Growth Des.*, 2010, **10**, 283; (*b*) L. F. Ma, Y. Y. Wang, L. Y. Wang, D. H. Lu, S. R. Batten and J. G. Wang, *Cryst. Growth Des.*, 2009, **9**, 2036; (*c*) M. H. Zeng, Y. L. Zhou, M. C. Wu, H. L. Sun and M. Du, *Inorg. Chem.*, 2010, **49**, 6436; (*d*) O. Kahn, *Molecular Magnetism*, VCH Publishers, New York, 1993; (*e*) J. S. Miller, M. Drillon, *Magnetism: Molecules to Materials I–V*, Wiley–VCH, Weinheim, Germany, 2001; (*f*) V. Laget, C. Hornick, P. Rabu, M. Drillon and R. Ziessel, *Coord. Chem. Rev.*, 1998, **178**, 1533.

30 (*a*) J. M. Rueff, N. Masciocchi, P. Rabu, A. Sironi and A. Skoulios, *Eur. J. Inorg. Chem.*, 2001, 2843; (*b*) P. Rabu, J. M. Rueff, Z. L. Huang, S. Angelov, J. Souletie and M. Drillon, *Polyhedron*, 2001, **20**, 1677; (*c*) J. M. Rueff, N. Masciocchi, P. Rabu, A. Sironi and A. Skoulios, *Chem.–Eur. J.*, 2002, **8**, 1813.

31 J. W. Raebiger, J. L. Manson, R. D. Sommer, U. Geiser, A. L. Rheingold and J. S. Miller, *Inorg. Chem.*, 2001, **40**, 2578.

32 F. Luo, Y. X. Che and J. M. Zheng, *Cryst. Growth Des.*, 2009, **9**, 1066.

